Available online at www.sciencedirect.com
SCIENCE DIRECT®
Vision Research 45 (2005) 1031–1045
Vision Research
www.elsevier.com/locate/visres

Chromatic assimilation: spread light or neural mechanism?

Dingcai Cao [a,b,c], Steven K. Shevell [b,c,*]

[a] Departments of Health Studies, University of Chicago, 940 East 57th Street, Chicago, IL, 60637, USA
[b] Departments of Ophthalmology and Visual Science, University of Chicago, 940 East 57th Street, Chicago, IL, 60637, USA
[c] Departments of Psychology, University of Chicago, 940 East 57th Street, Chicago, IL, 60637, USA

Received 8 July 2004; received in revised form 11 October 2004

Abstract

Chromatic assimilation is the shift in color appearance of a test field toward the appearance of nearby light. Possible explanations of chromatic assimilation include wavelength independent spread light, wavelength-dependent chromatic aberration and neural summation. This study evaluated these explanations by measuring chromatic assimilation from a concentric-ring pattern into an equal-energy-white background, as a function of the inducing rings' width, separation, chromaticity and luminance. The measurements showed, in the *s* direction, that assimilation was observed with different inducing-ring widths and separations when the inducing luminance was lower or higher than the test luminance. In general, the thinner the inducing rings and the smaller their separation, the stronger the assimilation in *s*. In the *l* direction, either assimilation or contrast was observed, depending on the ring width, separation and luminance. Overall, the measured assimilation could not be accounted for by the joint contributions from wavelength-independent spread light and wavelength-dependent chromatic aberration. Spatial averaging of neural signals explained the assimilation in *s* reasonably well, but there were clear deviations from neural spatial averaging for the *l* direction.

Keywords: Chromatic assimilation; Chromatic contrast; Spread light; Chromatic aberration; Neural summation

1. Introduction

The perceived color of a light is well known to depend not only on its spectral power distribution but also on other light nearby. The change in color appearance due to nearby light is called chromatic induction. There are two qualitatively different types of induction: chromatic contrast and chromatic assimilation. Chromatic contrast occurs when the color appearance of a test light shifts away from the color appearance of the nearby inducing light. Chromatic assimilation occurs when the appearance of the test light shifts toward the color appearance of inducing light.

Chromatic contrast has been studied extensively for more than 160 years (for example, Chevreul, 1839; Jameson & Hurvich, 1955; Shevell & Wei, 1998; von Kries, 1905; Ware & Cowan, 1982) but chromatic assimilation has received less attention. Assimilation was described in the 19th century by von Bezold (1876) and may, in fact, be more common than contrast (DeValois & DeValois, 1988). Powerful demonstrations of chromatic assimilation are given by Hurvich (1981) and Shevell (2003). The purpose of this study is to systematically measure chromatic assimilation and to assess the physiological mechanisms posited to mediate it.

1.1. Possible explanations for chromatic assimilation

The possible explanations for chromatic assimilation can be divided into two classes: non-neural and neural. Non-neural theories explain assimilation by changes

* Corresponding author. Address: Visual Science Laboratories, University of Chicago, 940 East 57th Street, Chicago, IL, 60637, USA. Tel.: +1 773 702 8842.
E-mail address: shevell@uchicago.edu (S.K. Shevell).

0042-6989/$ - see front matter © 2004 Elsevier Ltd. All rights reserved.
doi:10.1016/j.visres.2004.10.016

that occur in the retinal stimulus, prior to transduction. Explanations that involve neural mechanisms include retinal and cortical processes. Some neural theories account for assimilation in terms of receptive-field organization (DeValois & DeValois, 1975; Hurvich & Jameson, 1974; Monnier & Shevell, 2004) or tuned spatial filters (Blakeslee & McCourt, 1999). Other theories suggest assimilation depends on higher-level perceptual cues, such as the geometric structure of the stimulus, perceptual organization, figure/ground segregation, or perceptual grouping (de Weert & van Kruysbergen, 1997; Festinger, Coren, & Rivers, 1970; Taya, Ehrenstein, & Cavonius, 1995; Todorovic, 1997; Zaidi, Spehar, & Shy, 1997).

Non-neural explanations for assimilation include wavelength-independent spread light and wavelength-dependent chromatic aberration (Helson, 1963; Smith, Jin, & Pokorny, 2001; Wright, 1969). Non-neural factors can lead to assimilation because they change the quantal absorption within the retinal area of the test region. Wavelength-independent spread light is due to optical imperfections and scattered light. Wavelength-dependent chromatic aberration occurs because the lens of the eye refracts short-wavelength light more than long-wavelength light. A distant short-wavelength target is never exactly in focus on the retina (Kaiser & Boynton, 1996) so short-wavelength light is blurred in the retinal image.

Smith et al. (2001) estimate the contribution of wavelength-independent spread light to assimilation for an equiluminant square-wave grating, using a line-spread function developed by Williams, Brainard, McMahon, and Navarro (1994). Their calculations show that chromatic assimilation with their gratings may be accounted for by spread light. At the same time, they conclude that chromatic aberration is not a major source of assimilation at spatial frequencies at or below 9 cpd.

Wavelength-independent spread light and chromatic aberration undoubtedly contribute to chromatic assimilation. Numerous studies, however, conclude that chromatic assimilation cannot be accounted for entirely by these non-neural processes (de Weert & van Kruysbergen, 1997; Fach & Sharpe, 1986; Helson, 1963; Longere, Shevell, & Knoblauch, 2000). These studies strongly suggest that neural processes contribute to chromatic assimilation.

Neural spatial integration within receptive field centers is proposed to explain assimilation (DeValois & DeValois, 1975; Hurvich & Jameson, 1974; Jameson & Hurvich, 1989). In a repetitive stimulus pattern causing assimilation, neurons with small receptive fields may resolve the pattern but, simultaneously, responses from the same photoreceptors may drive other neurons with larger receptive fields that combine responses from nearby photoreceptors. The net response from a neuron with a larger receptive field can lead to assimilation. In a similar approach, de Weert and van Kruysbergen (1987) and de Weert (1991) propose that large receptive fields without center-surround antagonism account for assimilation. Assimilation would result from local averaging within these large receptive fields. Moulden, Kingdom, and Wink (1993) also propose neural summation to explain why a checkerboard consisting of alternating squares with complementary colors appears achromatic at higher spatial frequencies. Recent physiological evidence adds support to the proposal that there are two sets of neurons sensitive to chromatic information, one band pass and one low pass (Johnson, Hawken, & Shapley, 2001).

In contrast to models that incorporate neural responses from spatial filters, other investigators propose that assimilation is due to higher-level mechanisms of visual representation. For example, Fuchs (1923), King (1988) and Taya et al. (1995) argue that assimilation depends on object segmentation or perceptual belongingness. Other researchers posit that figure/ground segregation affects assimilation (de Weert & van Kruysbergen, 1997; Festinger et al., 1970).

While most studies agree that a neural process contributes to assimilation, the nature of the neural mechanisms remains unclear. The purpose of this study is to systematically investigate how chromatic assimilation varies with the width, separation, chromaticity and luminance of the inducer, using a stimulus pattern with both chromatic and luminance variation. These results rule out the possibility that spread light and chromatic aberration are a full explanation of chromatic assimilation, and support the view that neural summation contributes to chromatic assimilation.

2. Methods

2.1. Apparatus

All stimuli were displayed on a calibrated, high-resolution (1360×1024) color 21-inch Sony Trinitron CRT, which was controlled by a Macintosh G4 computer with a 10-bit Radius video board. The refresh rate was 75 Hz noninterlaced. The stimuli on the CRT were viewed haploscopically at a viewing distance of 1.15 m. The stimulus on the right side of the CRT screen was projected to the right eye and the stimulus on the left side of the CRT screen to the left eye. An adjustable chin rest maintained the observer's head position.

2.2. Stimuli

A test field and a uniform matching field were steadily presented through the haploscope (Fig. 1a). The uniform matching field was viewed by the observer's right eye. Its diameter was 3°. The test field, viewed by the ob-

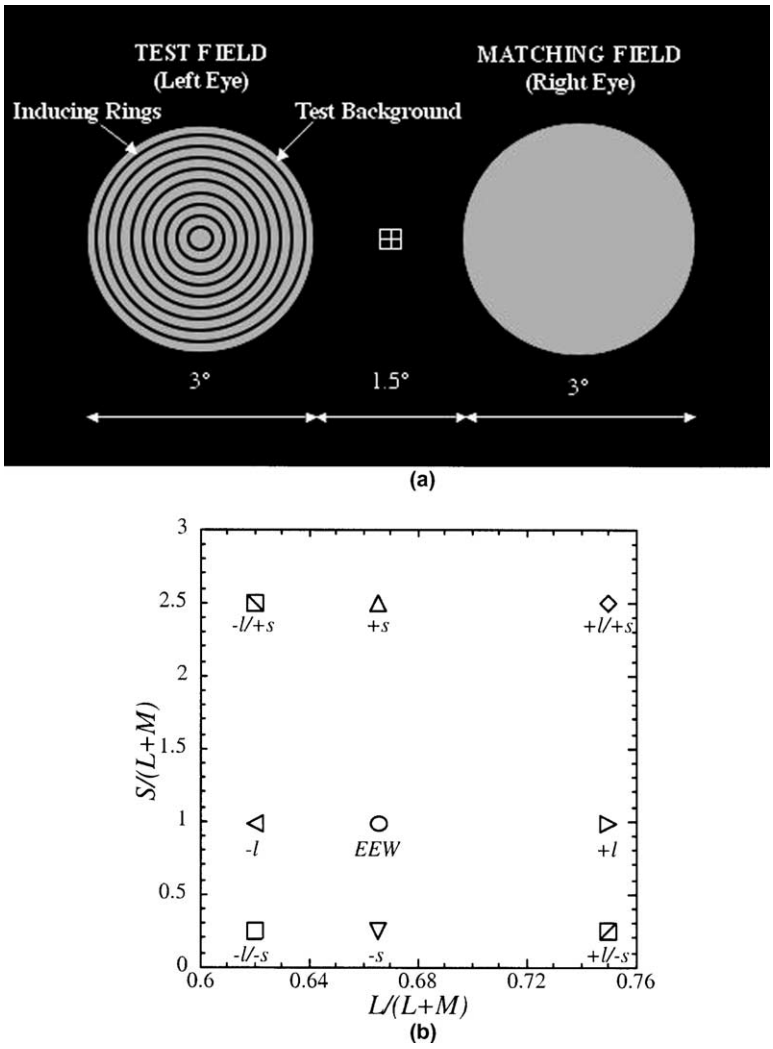

Fig. 1. (a) The haploscopically presented stimuli. The 3° uniform matching field was presented to the observer's right eye. The test field, presented to the observer's left eye, was composed of a background with concentric inducing rings. (b) The chromaticities of the background (EEW) and inducers in a modified MacLeod and Boynton (1979) cone space.

server's left eye and also 3° in diameter, was composed of a background presented with concentric inducing rings. The background was judged in color. The width of the inducing rings was 1, 2 or 4 min. The separation between the rings also was varied: 2, 4, 8, or 16 min. With these combinations of ring width and separation, the spatial frequencies covered a range from 3 to 20 cpd.

The chromaticities of the inducing rings and of the background serving as the test field are shown in Fig. 1b. The chromaticity of the background, which was essentially metameric to equal-energy-white (EEW), had coordinates *l*, *s* of 0.665, 0.99 in this modified MacLeod and Boynton (1979) diagram, in which *s* for EEW is 1.00. The luminance of the background was 4 cd/m^2. The inducing chromaticities were labeled "+*l*", "−*l*", "+*s*", "−*s*", "+*l*/+*s*", "+*l*/−*s*", "−*l*/+*s*" and "−*l*/−*s*", which were named by their *l* and *s* chromaticities relative to EEW. For instance, the "+*l*/+*s*" inducing rings had higher values of *l* and *s* than the EEW background. These inducing chromaticities formed a rectangle in the cone space. The luminance of the inducing rings was varied: either 2.67 or 6.0 cd/m^2. The corresponding Michelson contrast with respect to the test was 0.20 for both luminances.

2.3. Procedure

The method of haploscopic matching was used to measure chromatic assimilation. During the experiment, the width, separation, chromaticity, and luminance of the inducing rings were varied. In each session, one width and one separation were selected randomly. Each combination of inducer chromaticity and luminance was replicated 2 times in one session. The chromaticities and luminances of the inducing rings were randomly ordered. The starting chromaticity of the matching field

was randomly chosen from the CRT color gamut. To match the color of the background in the test field, an observer adjusted the hue, saturation and brightness of the matching field via a multi-button game pad sensed by the computer. When the observer was satisfied with the match, he or she pressed a confirmation button on the game pad, which recorded the response and initiated the next trial.

The measurements were conducted in a dark room. Before each session, the observer dark-adapted for three minutes. The measurements were replicated on four different days. The order of sessions was randomized. The two measurements for each condition within each session were averaged and recorded as the match from that session. The means and standard errors of the matches were determined from the match value from each of four sessions on different days.

2.4. Observers

Three observers participated in the study: XM (female), DC (male), and ZX (female). These observers had an age range from 25 to 33 years. Each observer had normal color vision as evaluated by a Neitz anomolascope. Observer DC, one of the authors, was an experienced psychophysical observer. The other observers were naïve regarding the design and purpose of this study. Each observer signed a consent form before participating in this study. The experimental procedures were approved by an Institutional Review Board at the University of Chicago.

For each observer, a minimum motion technique (Anstis & Cavanagh, 1983) was used to achieve equiluminance of each phosphor of the color CRT. The luminance of each stimulus for each observer was adjusted using these minimum-motion measurements. Also, a minimally distinct border technique (Tansley & Boynton, 1978) was used to verify that each observer's tritan line did not deviate significantly from theoretical values that isolate S cones.

2.5. Model: Wavelength-independent spread light and chromatic aberration

Wavelength-independent spread light and chromatic aberration were modeled based on the method of Marimont and Wandell (1994), which incorporates the wavelength-independent spread light function from Williams et al. (1994) with the wavelength-dependent optical transfer function of a model eye for a given pupil size. Because of the relatively small inducing-ring widths used in this study (1, 2 and 4 min), the spatial resolution of the point spread function used for calculations was approximately 0.2 min per pixel. The pupil diameter was set to 3.6 mm, which is the pupil size at 4 cd/m^2 given by Degroot and Gebhard (1952). For each stimulus, with inducing rings of given width, separation, chromaticity and luminance, the spectral distribution in each spatial location of the physical stimulus was calculated based on the spectral distributions of the R, G, and B guns of the CRT. The resulting spatial distribution of light at each wavelength was convolved with the point-spread function at that wavelength. The average retinal chromaticity was calculated for the central 1 min region within each band of the test (that is, between each pair of adjacent inducing rings), and used as the theoretically predicted chromaticity resulting from the joint contributions from wavelength-independent spread light and chromatic aberration.

2.6. Model: Spatial averaging of neural signals

Suppose the neural response from an inducing light I, with chromaticity (l_I, s_I) and luminance LUM_I, is any (possibly nonlinear) function $f_I(l_I, s_I, \mathrm{LUM}_I)$; and the neural response for the test (background) light T, with chromaticity (l_T, s_T) and luminance LUM_T, is any function $f_T(l_T, s_T, \mathrm{LUM}_T)$ (Shevell & Cao, 2003). For a given stimulus composed of a particular set of inducing rings and background (as in Fig. 1a), the proportion of the whole stimulus area covered by the inducing light, P, is a function of the width of the inducing rings and the separation between successive inducing rings. The weighted spatial average of the neural responses, $\mathrm{SA}(P)$, is

$$\begin{aligned}\mathrm{SA}(P) &= P\theta f_I(l_I,s_I,\mathrm{LUM}_I) + (1-P) f_T(l_T,s_T,\mathrm{LUM}_T)\\ &= f_T(l_T,s_T,\mathrm{LUM}_T) + P[\theta f_I(l_I,s_I,\mathrm{LUM}_I)\\ &\qquad - f_T(l_T,s_T,\mathrm{LUM}_T)]\\ &= \mathrm{SA}(0) + P[\mathrm{SA}(1) - \mathrm{SA}(0)], \end{aligned} \tag{1}$$

where θ is the weight of the neural response from the inducing light that contributes to the spatial average. If summation were complete, then the value of θ would be 1.0; otherwise, θ would be less that 1.0. Notice that Eq. (1) uses the facts that $\mathrm{SA}(0) = f_T(l_T, s_T, \mathrm{LUM}_T)$ (no inducing light) and $\mathrm{SA}(1) = \theta f_I(l_I, s_I, \mathrm{LUM}_I)$ (no test light). Eq. (1) implies that the spatial average of the neural response is a linear function of the proportion of the stimulus area covered by the inducing light. Moving the term SA(0) in Eq. (1) to the left side gives

$$\mathrm{SA}(P) - \mathrm{SA}(0) = P[\mathrm{SA}(1) - \mathrm{SA}(0)]. \tag{2}$$

For a stimulus pattern with a fixed size, inducing-ring width, chromaticity and luminance of the test and inducing lights, a direct test of Eq. (2) is to alter the separation between inducing rings, which changes only P. If the measured change, $\mathrm{SA}(P) - \mathrm{SA}(0)$, is a linear function of P, then a weighted average of (perhaps nonlinear) neural signals would be supported. A parameter free test of the spatial averaging of neural responses can be achieved by substituting $P_{\max}$ for P in Eq. (2)

and then using the measured shift for the same ring width with the largest proportion (P_{max}) of stimulus area covered by the inducing light: [SA(P_{max}) − SA(0)]. Then

$$\frac{SA(P) - SA(0)}{SA(P_{max}) - SA(0)} = \frac{P[SA(1) - SA(0)]}{P_{max}[SA(1) - SA(0)]} = \frac{P}{P_{max}}. \quad (3)$$

Eq. (3) shows that the normalized value $\left(\frac{SA(P)-SA(0)}{SA(P_{max})-SA(0)}\right)$ equals the normalized proportion of the inducing area $\left(\frac{P}{P_{max}}\right)$, which implies that the normalized shift in color appearance plotted as a function of the normalized proportion of the inducing area should fall on a straight line that has unit slope and that passes through the origin.

Note that Eq. (3) does not specify the chromatic pathway affected by the neural signals. The neural response, therefore, can be $l = L/(L + M)$ or $s = S/(L + M)$ so Eq. (3) applies to l or s. Thus, the spatial averaging model can be tested for either pathway.

3. Results

3.1. Overview of the experiments

Assimilation was measured in 176 experimental conditions for each observer: 8 inducing chromaticities, 2 inducing luminances and 11 ring-width-and-separation combinations. The matching results with the 2 min wide inducing rings at 2.67 cd/m^2 for observer XM are shown in Fig. 2. In the figure, the matching $l = L/(L + M)$ for the "$+l/+s$", "$+l$", "$+l/-s$", "$-l/+s$", "$-l$" and "$-l/-s$" inducing rings at different separations are shown in the upper panel and the matching $s = S/(L + M)$ for "$+l/+s$", "$+s$", "$-l/+s$", "$+l/-s$", "$-s$" and "$-l/-s$" in the lower panel. Within each panel, the matching l or s value for each inducing chromaticity is shown by the same symbol as in Fig. 1b. The horizontal dashed line shows isomeric matching for l or s to the "EEW" background.

Compared to the isomeric matches to the "EEW" background (no inducing rings), the magnitude of the shifts in l with the "$+l/+s$", "+l" and "$+l/-s$" inducing rings at various separations was very similar: at 2 min separation, large shifts in l toward the inducing chromaticity were observed; at larger separations (4, 8 and 16 min), however, the shifts in l were near zero. The magnitude of the shifts in l with the "$-l/+s$", "$-l$" and "$-l/-s$" inducing rings was also similar: the shift in l was toward the inducing chromaticity at all the separations; further, the shift in l became smaller with larger separations.

With the "$+l/+s$", "$+s$" and "$-l/+s$" inducing rings, large shifts in s toward the inducing chromaticity were observed at all separations; further, the shifts in s decreased with the increase in the separation. With the "$+l/-s$", "$-s$" and "$-l/-s$" inducing rings, the shift in s toward the inducing chromaticity was observed only at the 2 min separation; at other separations, the shifts in s were minimal.

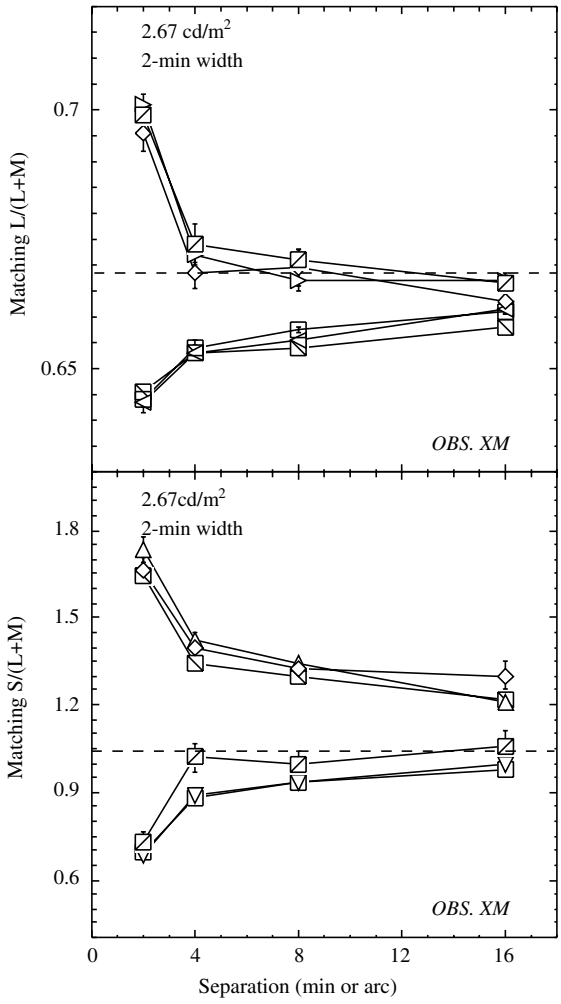

Fig. 2. The matching results with the 2-min wide inducing rings at 2.67 cd/m^2 for observer XM. The symbols used for different inducing chromaticities are the same as those in Fig. 1b.

The complete set of matching measurements for observer XM is shown in Fig. 3 for the matching l settings and in Fig. 4 for the matching s settings. In the figures, the left (right) column shows the matching results at 2.67 (6.0) cd/m^2. As expected, the shifts in l or s depended on the inducing-ring luminance, the width and separation. Specifically, at the lower luminance (left column), the shift in l was toward the chromaticity of the inducing rings or was near zero. The magnitude of shift was smaller with larger separation for a given ring width. At the higher luminance (right column), the shift in l toward the chromaticity of the inducing rings was observed only with the 2 min separation. When the separation was larger than 2 min, the shift in l was away from the chromaticity of the inducing rings; that is, chromatic contrast was observed with larger separation.

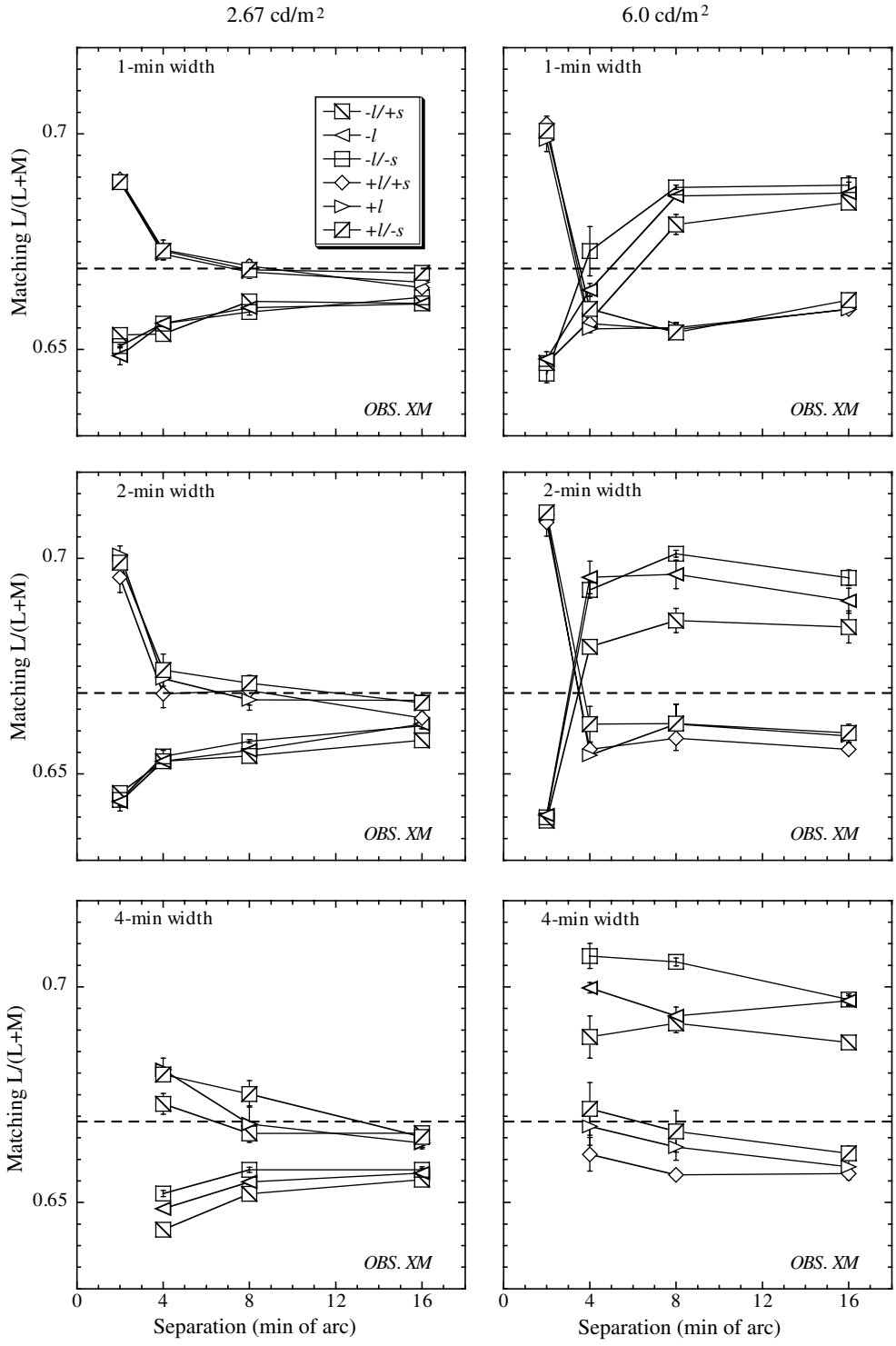

Fig. 3. Matching *l* values with different inducing-ring width-and-separation combinations, chromaticities and luminances for observer XM. The symbols used for different inducing chromaticities are the same as those in Fig. 1b.

The pattern of the shift in *s* was different from that of the shift in *l*. At both luminances, the shift in *s* was in the direction of assimilation or near zero. At the lower luminance, the larger the separation, the smaller the shift in *s*. At the higher luminance, however, the shift in *s* was nearly constant when separation was 4 min or more.

Fig. 3 shows the similarity among the matching *l* settings with inducing chromaticities that had higher *l* chromaticities than the background judged in color

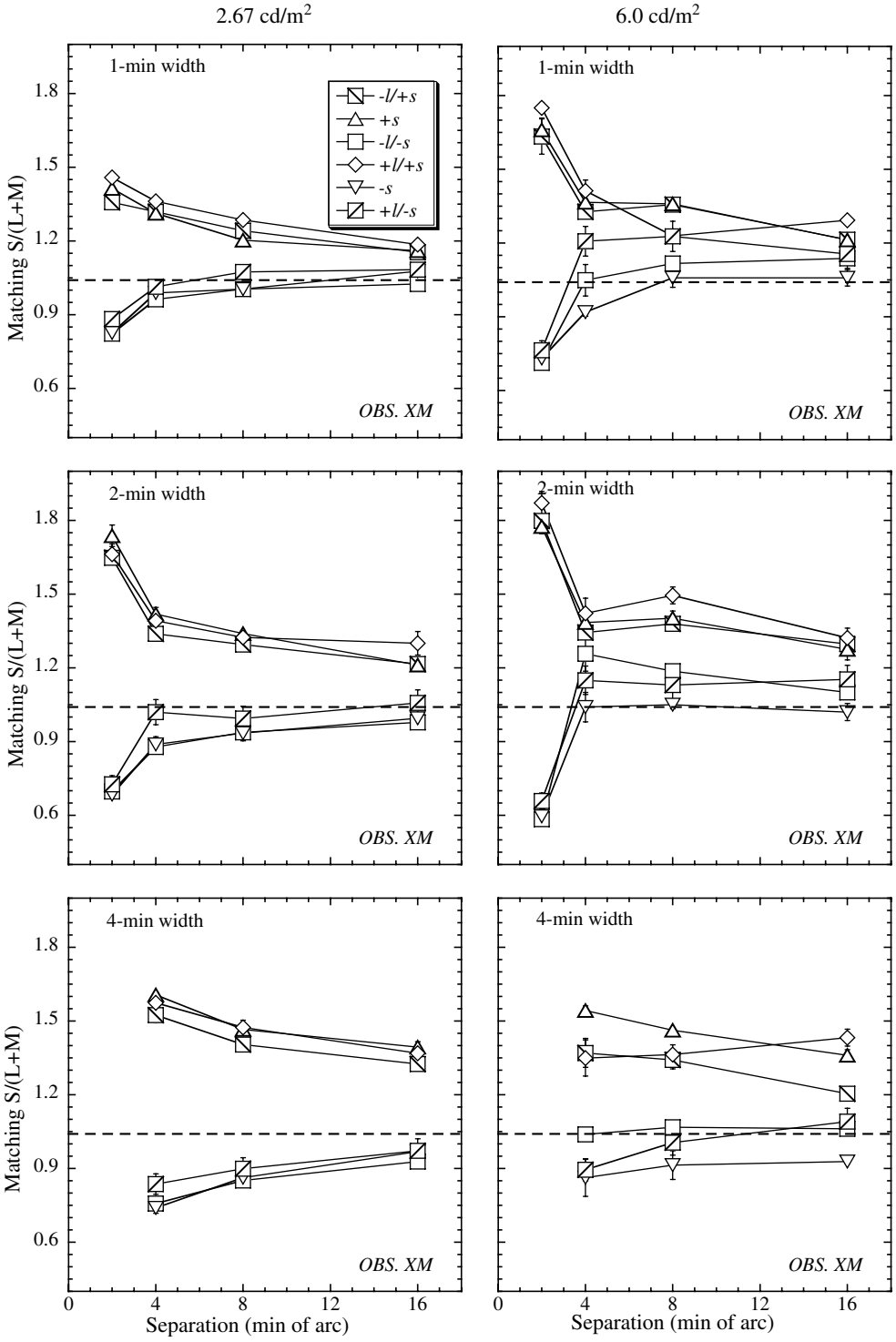

Fig. 4. As Fig. 3, for matching *s* values.

("higher *l*" group: "+*l*/+*s*", "+*l* " and "+*l*/−*s*"). The similarity of the matching *l* settings with the "+*l*/+*s*", "+*l*" and "+*l*/−*s*" inducer was observed also for the two other observers. Therefore, the matching *l* settings with the "+*l*/+*s*", "+*l*" and "+*l*/−*s*" inducing rings at each inducing width, separation and luminance were averaged for each observer. Similarly, the matching *l* with the "−*l*/+*s*", "−*l*" and "−*l*/−*s*" inducing rings ("lower *l*" group), the matching *s* with the "+*l*/+*s*", "+*s*" and "−*l*/+*s*" rings ("higher *s*" group), and the matching *s* with the "+*l*/−*s*", "−*s*" and "−*l*/−*s*" rings ("lower *s*" group) were averaged for each observer.

The averaged shifts in l and s relative to isomeric matches for all three observers are shown in Figs. 5 and 6, respectively. In the figures, the left column shows results with the inducing rings at 2.67 cd/m^2 and the right column shows results at 6.0 cd/m^2. Each panel is labeled with the width of the inducing rings. The average shifts for the "higher l", "lower l", "higher s", and "lower s" groups for each observer are labeled with different symbols.

The patterns of shifts in l were similar for all three observers (Fig. 5). At the lower inducing luminance (2.67 cd/m^2), the shift in l was toward the inducing chro-

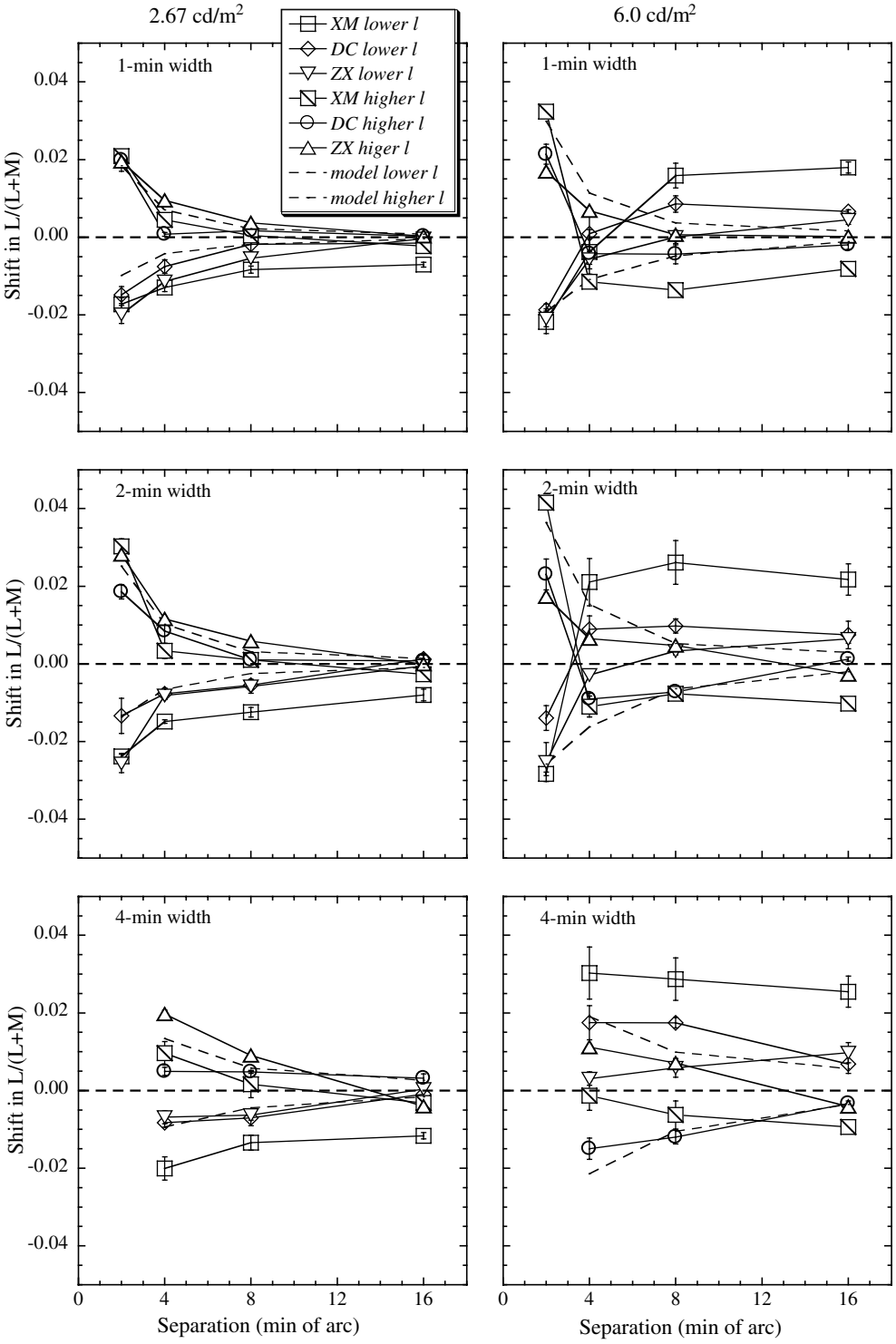

Fig. 5. The matching l values for observers XM, DC and ZX. The matching results were averaged to form the "higher l" and "lower l" chromaticity groups (see text).

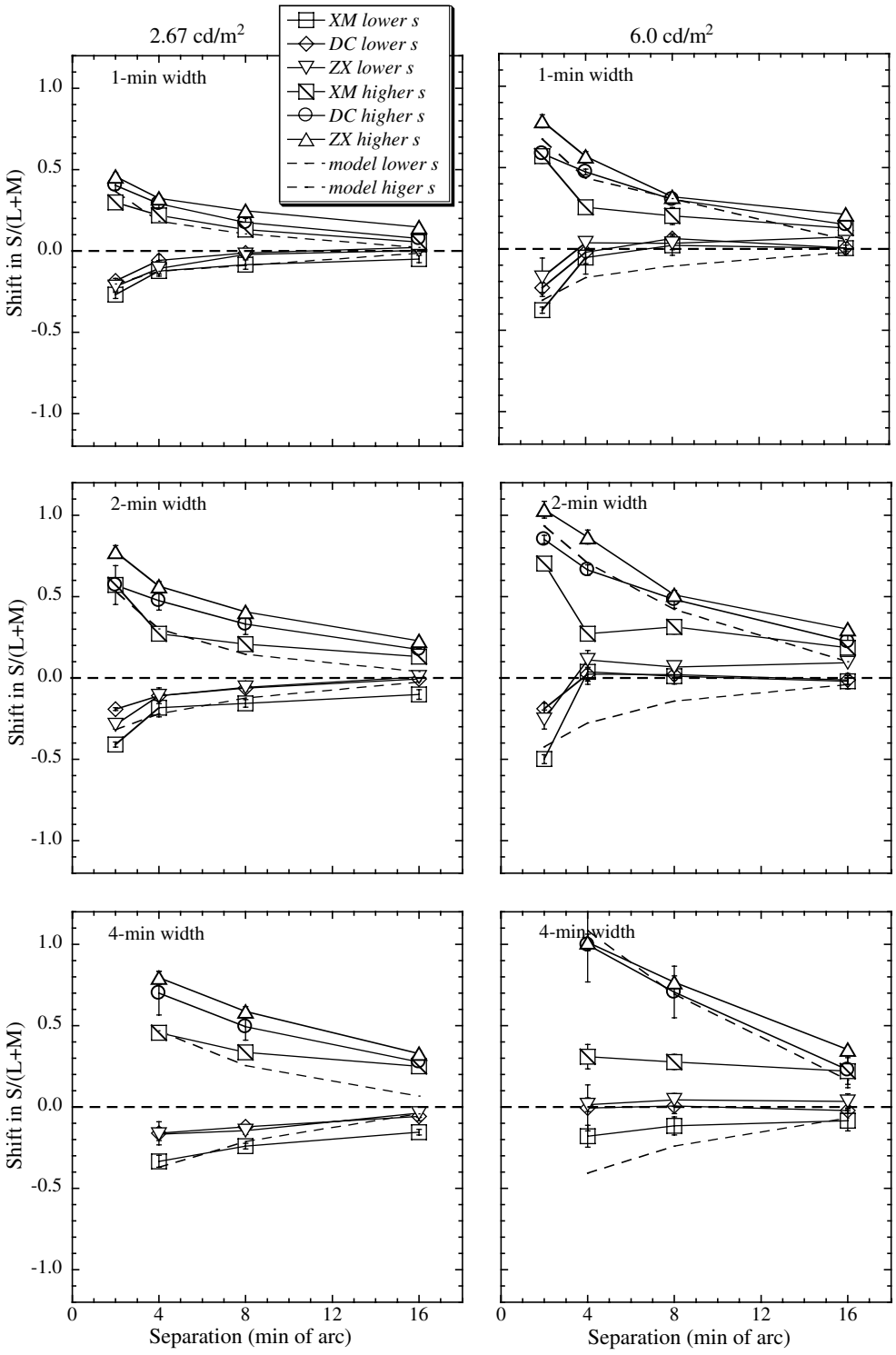

Fig. 6. As Fig. 5 but for matching *s* values for the "higher *s* " and "lower *s* " chromaticity groups (see text).

maticity or near zero. Stronger assimilation in *l* was observed with smaller separations. At the higher inducing luminance level (6.0 cd/m^2), chromatic contrast was observed with larger separations (larger than 2 min for observers XM and DC), though the observed contrast was weaker for observer ZX.

For all observers, the shift in *s* with either " higher *s* " or "lower *s* " inducing lights was generally toward the inducing chromaticity, or else near zero (Fig. 6). For the "higher *s* " group, the assimilation was stronger in *s* with smaller separation. This generally held at both inducing luminances (2.67 or 6.0 cd/m^2) for each ring

width (1, 2 or 4 min). For the "lower *s*" group, clear assimilation was observed only at smaller separations (2 or 4 min).

Overall, assimilation in *l* or *s* was stronger with higher spatial frequency. Further, assimilation in *l* was consistently found when the inducing luminance was lower than the test luminance but not when it was higher. This finding corroborates a similar observation reported by de Weert and Spillmann (1995).

3.2. Wavelength-independent spread light and chromatic aberration

The predicted results from wavelength-independent spread light and chromatic aberration for the "higher *l*" and "lower *l*" groups and for the "higher *s*" and "lower *s*" groups are also shown in Figs. 5 and 6 (dashed lines). With the "higher *l*" group at 2.67 cd/m^2, the predicted *l* shifts from optical factors were close to the measured values. With the "lower *l*" group at 2.67 cd/m^2, however, the predicted shifts in *l* were often smaller than the measured shifts in *l*. At 6.0 cd/m^2, the predicted shifts in *l* could not be meaningfully compared to the measurements in most conditions because contrast in *l* was observed.

With the "higher *s*" group at 2.67 cd/m^2 (left column, Fig. 6), the predicted shifts in *s* due to optical factors were consistently smaller than the measured shifts in *s*; with the "lower *s*" group at 2.67 cd/m^2, the predicted *s* values corresponded to the measurements reasonably well. At 6.0 cd/m^2, the predicted *s* settings were generally as large or larger than the measured *s* values.

The fraction of light spreading from the inducing field into the test field is independent of inducing luminance, for any given stimulus pattern with a fixed inducing-ring width, separation and chromaticity. If wavelength-independent spread light and wavelength-dependent chromatic aberration fully account for assimilation, the ratio of color shifts at two inducing luminances with the same stimulus pattern can be calculated using the method of Marimont and Wandell (1994). As contrast in *l* was observed at the higher luminance (6.0 cd/m^2) and the shift in *s* with the "lower *s*" chromaticity group was weak, the ratio of the measured shifts at the two luminances was calculated for only the "higher *s*" chromaticity group. Fig. 7 shows the ratios of the measured shifts in *s* at the two inducing luminances for the "higher *s*" chromaticity group, for inducing rings 1, 2, and 4 min wide (top, middle and bottom panel, respectively). At 2-min separation, the ratios with 1 and 2 min-wide inducing rings were close to the calculated ratio (leftmost points in the top and middle panels). For other conditions, all the measured ratios were far smaller than the corresponding calculated ratios. This was due primarily to the shifts at the lower luminance (2.67 cd/m^2), which

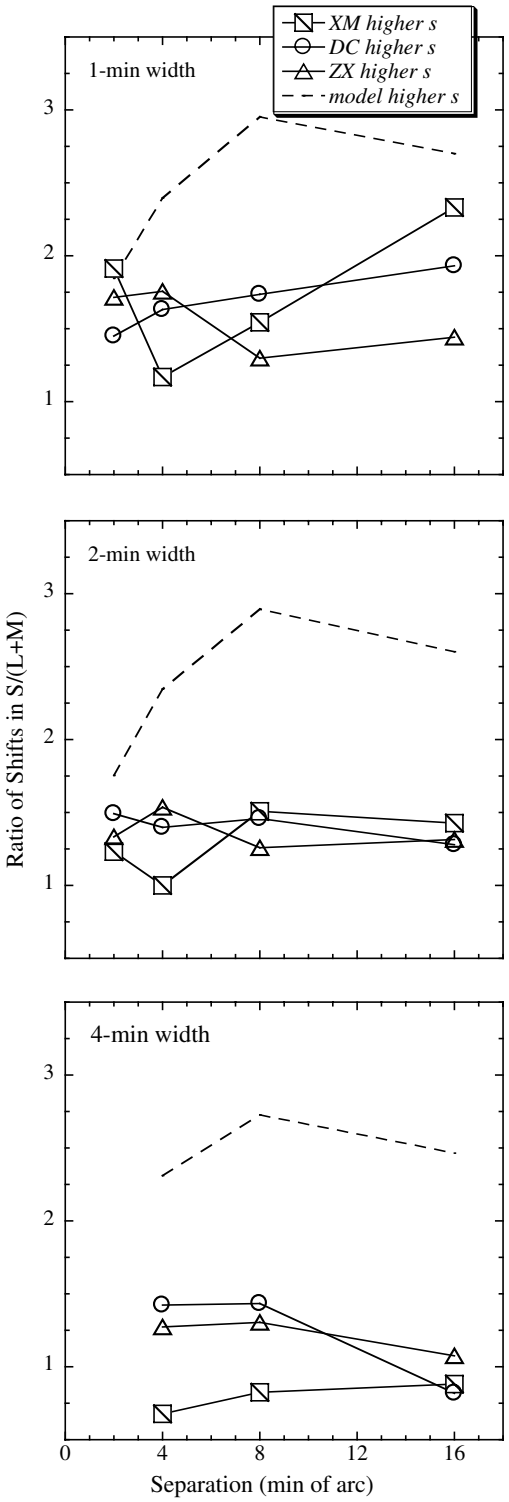

Fig. 7. The ratio of the shifts in *s* at the two luminances, for the "higher *s*" chromaticity group.

were larger than predicted by optical factors for most of the "higher *s*" conditions (left panels, Fig. 6).

In sum, the measured assimilation with the lower luminance "higher *s*" inducing rings (2.67 cd/m^2) could not be accounted for by wavelength-independent spread light and chromatic aberration. The discrepancy be-

tween the predicted and measured ratios at the two luminances followed from the failure of optical factors to account for assimilation at the lower luminance, not from a discrepancy at the higher inducing luminance.

3.3. Spatial averaging of neural signals in chromatic pathways

Spatial averaging of neural signals in chromatic pathways (Eq. 3) implies a precise empirical relation when inducing light of fixed width, chromaticity and luminance is varied with respect to the proportion of total area coved by the inducing light. Specifically, the shift in l or s with inducing-area proportion P, SA(P) − SA(0), normalized by the shift in l or in s at the maximum inducing-area proportion P_{max} used in the experiment, SA(P_{max}) − SA(0), is equal to the inducing-area proportion P divided by P_{max}. To test the spatial averaging model, for each ring width of 1, 2 or 4 min, the shift in l or s with the "higher l", "lower l",

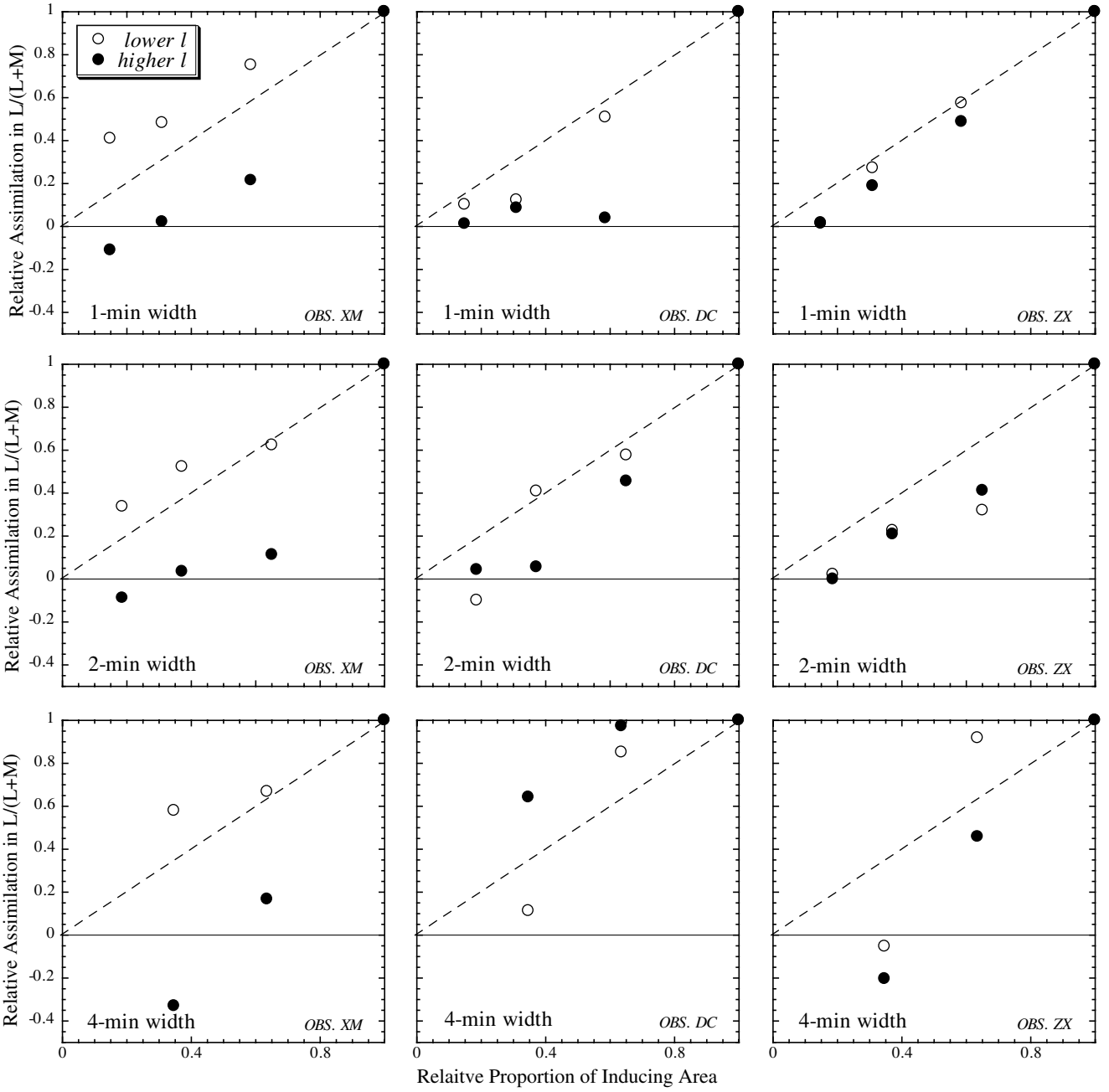

Fig. 8. Normalized shifts in l for the "higher l" and "lower l" inducing rings at ring widths of 1, 2, and 4 min. Results from each observer are shown in a separate column.

"higher *s*" or "lower *s*" inducing rings at 2.67 cd/m^2 was normalized by the shift with the smallest separation for that ring width (that is, the shift for P_{max}). This ratio was compared to the relative area covered by inducing light (P/P_{max}). Figs. 8 and 9 show the normalized shifts in *l* and *s*, respectively, plotted as a function of the relative inducing-light area, which for neural spatial averaging should follow a straight line of slope 1.0 through the origin (dashed lines in figures). The measured shifts with inducing rings at 6.0 cd/m^2 were not considered because chromatic contrast was found with the "higher *l*" or "lower *l*" inducing rings at some ring-width-and-separation combinations.

For the 1 or 2 min wide "lower *l*" inducing rings at 2.67 cd/m^2 (open circles in top and middle rows, Fig. 8), the predicted linear relation was a reasonable approximation of the results. For the "higher *l*" group (filled circles), large deviations from the predictions based on neural spatial averaging were evident for nearly all conditions and all observers.

The normalized shifts in *s* (Fig. 9) were described by the spatial averaging model better than the shifts in *l*

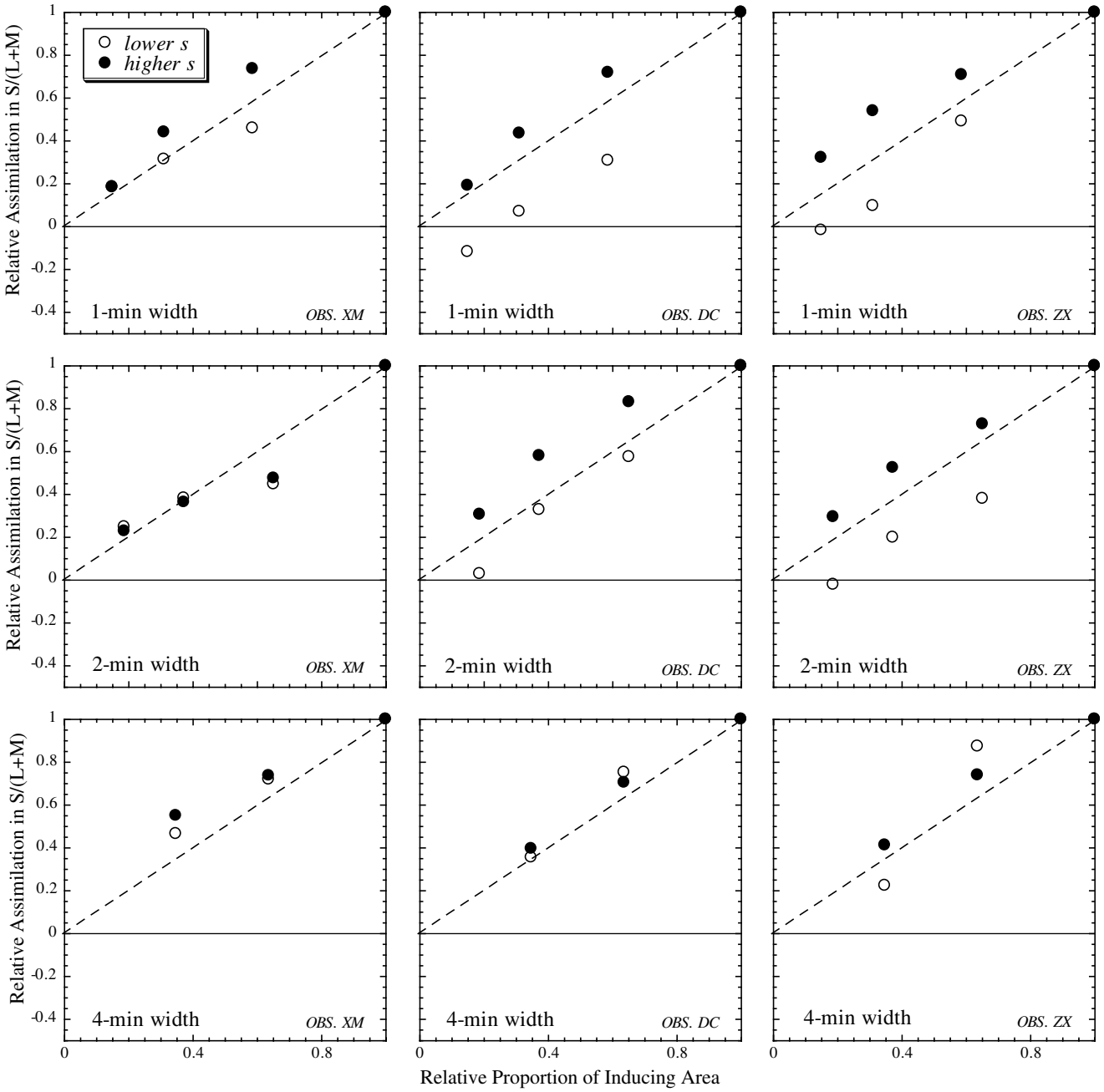

Fig. 9. As Fig. 8 but for normalized shifts in *s* for the "higher *s*" and "lower *s*" inducing rings.

and, overall, spatial averaging explained a substantial portion of the variance in *s*. Excluding the data points in Fig. 9 at value 1.0, which were pinned to this value by normalization, the percentage of the variance in the normalized shifts explained by the predicted line in the "higher *s*" and "lower *s*" conditions (pooled for 1, 2, and 4 min wide inducing rings) was 94%, 90%, and 88% for observers XM, DC and ZX, respectively (these values maintained the intercept at zero so total variance was not corrected for the mean). Recall that the predictions for neural spatial averaging have no free parameters; the dashed lines in Fig. 9 were not fit to the measurements.

A linear regression with a constraint of zero intercept was fit to the relative shifts as a function of the normalized proportion of inducing area, for each inducing width, chromaticity ("higher *l*", "lower *l*", "higher *s*" and "lower *s*"), and observer. With the "higher *s*" and "lower *s*" inducing rings, the best fitting slopes were close to 1.0, which was the predicted slope for neural spatial averaging: the mean value of the slope across the inducing widths (1, 2 and 4 min) with the "higher *s*" and "lower *s*" inducing rings was 1.02 ± 0.07 for XM, 1.03 ± 0.09 for DC, or 1.02 ± 0.10 for ZX. The fitted slopes with the "higher *l*" and "lower *l*" inducing rings, however, were considerably less than 1.0, and variation across inducing widths was relatively large for each observer: the mean value of the slope across the inducing widths was 0.67 ± 0.17 for XM, 0.84 ± 0.14 for DC, and 0.69 ± 0.11 for ZX. Overall, therefore, the color shifts from assimilation were accounted for fairly well by neural spatial averaging for the "higher *s*" and "lower *s*" inducing rings, but not for the "higher *l*" and "lower *l*" inducing rings.

4. Discussion

At both inducing luminances and for any inducing-ring width, chromatic assimilation in *l* or *s* was strongest with the narrowest separation. This was consistent with previous reports that chromatic assimilation occurs with relatively fine gratings or high spatial frequencies (Fach & Sharpe, 1986; Helson, 1963; Smith et al., 2001; Walker, 1978). Fach and Sharpe (1986) and Smith et al. (2001) show that spatial frequency is a major factor determining the transition from chromatic assimilation to chromatic contrast. With the ring width and separation combinations used here, the spatial frequency covered a range from 3 cpd to 20 cpd. The transition from assimilation to contrast would be expected for both luminances if spatial frequency were the only factor determining the transition.

At the lower inducing luminance here (2.67 cd/m^2, which was less than the test luminance of 4.0 cd/m^2), no transition from assimilation to contrast was evident. At the higher inducing luminance (6.0 cd/m^2), there was a qualitative difference between the induced color shifts in the *l* and *s* directions: in the *s* direction, assimilation was always observed; in the *l* direction, however, there was a transition from assimilation to contrast. Unlike experiments conducted by Fach and Sharpe (1986) and Smith et al. (2001), which used equiluminant stimuli, our experiments employed a stimulus pattern with both luminance contrast and chromatic contrast between the inducing and test lights. The results here show that luminance contrast plays an important role in the transition from assimilation to contrast.

Wavelength-independent spread light and chromatic aberration can contribute to chromatic assimilation. Smith et al. (2001) report their measured assimilation with equiluminant square-wave gratings at 9 cpd can be explained by spread light. The conditions studied here, with stimulus patterns with both chromatic and luminance contrast between the inducing and test fields, were more general. The comparison of the measured assimilation and the predicted assimilation from optical factors, based on Marimont and Wandell (1994), demonstrated that wavelength-independent spread light and wavelength-dependent chromatic aberration could not fully account for the measured assimilation. This implicates a neural contribution to assimilation.

One other possible non-neural factor that might explain assimilation also can be excluded: light scatter within the CRT video display. Assuming this internal scatter for a given chromaticity is proportional to luminance, two separate estimates of the proportion of internal scatter can be calculated from the two color-appearance measurements at inducing luminances 2.67 and 6.0 cd/m^2 (Cao, 2003). These two estimates can be used to test the null hypothesis that the proportion of internally scattered light is the same at both inducing luminances, as required if the color shifts were due to internal scatter. A separate Wilcoxon non-parametric rank sum test (Rice, 1995) was completed for each observer at every combination of inducing width, separation and chromaticity, except when a measurement revealed contrast (which cannot be explained by scatter) or the induced color shift was very small (in which case a reliable estimate of the scatter proportion was not possible). Table 1 shows the total number of Wilcoxon tests done for each observer and the number of such tests that rejected the null hypothesis at 5% Type I error

Table 1
Summary of nonparametric statistical tests for internal display scatter

Observer	Wilcoxon rank sum tests	
	Number of tests	Number of tests rejected
DC	15	13
XM	19	14
ZX	23	15

(i.e., $\alpha = 0.05$). Over all three observers, 57 tests could be completed of which 42 rejected the null hypothesis (chance rejection frequency is 3 (5%) of 57 tests). Internal display scatter, therefore, cannot account for the chromatic assimilation found here.

Spatial averaging of (perhaps nonlinear) neural signals accounted fairly well for the measured assimilation in the *s* chromatic direction. Neural spatial summation has been proposed to occur in the centers of center-surround receptive fields (DeValois & DeValois, 1975; Hurvich & Jameson, 1974). Receptive-field organization may account for the transition from chromatic assimilation to contrast. Suppose spatial averaging of neural signals in a chromatic pathway occurs in the center of a receptive field with a fixed size. Then the transition from chromatic assimilation to contrast would be expected as the inducing rings become wider and fall outside of the center of the receptive field, as occurs at lower spatial frequencies or with a larger separation between the inducing rings. At the higher luminance, contrast was observed in *l* but not in *s*, which suggests a difference in the size of the receptive field in the *l* and *s* pathways. This is consistent with the larger receptive field in the *s* pathway than in the *l* pathway (Dacey & Lee, 1994). At the lower inducing luminance level, however, no contrast in *l* was observed with wider inducing rings at larger separation. One possibility is that the size of the receptive field that integrates signals in the *l* pathway is larger when the inducing luminance is lower than the test luminance, compared to when the inducer is higher in luminance than the test. de Weert and Spillmann (1995) report chromatic assimilation only when the luminance of the inducing pattern is lower than the test field. Clearly, luminance contrast between the inducing and test fields is an important factor affecting chromatic assimilation.

The assimilation in *s* can be modeled by a receptive field with S-cone spatial antagonism. In addition to S-ON bistratified ganglion cells (Dacey & Lee, 1994), there is a second class of ganglion cell with negative S-cone input in macaque (Dacey, D. M., personal communication). These S-OFF cells have about twice the diameter of S-ON bistratified cells. A central neural combination of signals from S-ON and S-OFF cells could establish a "$+s/-s$" receptive field. The measurements of *s* here were fit with a hypothetical "$+s/-s$" receptive field, with an excitatory response to $s = S/(L + M)$ in the center and an inhibitory response to *s* in the surround. The "$+s/-s$" receptive field was implemented as a difference of two Gaussians, one for the center and the other for the surround. The size of the surround was set to twice the size of the center. Using the calculated retinal image based on wavelength-independent spread light and chromatic aberration from Marimont and Wandell (1994), the optimal receptive field size was determined by minimizing squared errors between the response from the receptive field and the measurements from the "higher *s*" inducing condition (ring width 1, 2 and 4 min). Each observer was analyzed separately. The modeling showed the optimal receptive field size had a peak spatial frequency of 0.65 cpd for observer XM, 0.74 cpd for observer DC, and 0.76 cpd for observer ZX. These results for the three observers are consistent with the spatial frequency tuning for S-cone isolated vision (Humanski & Wilson, 1992), which includes one mechanism with peak sensitivity near 0.70 cpd.

Acknowledgments

This research was supported by NIH grant EY-04802. Publication was supported in part by an unrestricted grant to the Department of Ophthalmology and Visual Science from Research to Prevent Blindness.

References

Anstis, S., & Cavanagh, P. (1983). A minimum motion technique for judging equiluminance. In J. D. Mollon & L. T. Sharpe (Eds.), *Colour Vision Physiology and Psychophysics* (pp. 155–166). London: Academic Press.

Blakeslee, B., & McCourt, M. E. (1999). A multiscale spatial filtering account of the White effect, simultaneous brightness contrast and grating induction. *Vision Research, 39*, 4361–4377.

Chevreul, M. E. (1839). *The principles of harmony and contrast of colors and their applications to the arts. Original English translation, 1854, republished, 1967*. New York: Reinhold.

Cao, D. (2003). Chromatic assimilation. Doctoral dissertation, University of Chicago.

Dacey, D. M., & Lee, B. B. (1994). The 'blue-on' opponent pathway in primate retina originates from a distinct bistratified ganglion cell type. *Nature, 367*, 731–735.

de Weert, C. M. M. (1991). Assimilation versus contrast. In A. Valberg & B. B. Lee (Eds.), *From pigments to perception: Advances in understanding visual processes* (pp. 305–311). New York: Plenum.

de Weert, C. M. M., & Spillmann, L. (1995). Assimilation: Asymmetry between brightness and darkness? *Vision Research, 35*, 1413–1419.

de Weert, C. M. M., & van Kruysbergen, M. A. W. H. (1987). Subjective contour strength and perceptual superimposition: Transparency as a special case. In S. Petry & G. Meyer (Eds.), *The perception of illusory contours* (pp. 165–170). New York: Springer.

de Weert, C. M. M., & van Kruysbergen, M. A. W. H. (1997). Assimilation: Central and peripheral effects. *Perception, 26*, 1217–1224.

Degroot, S. G., & Gebhard, J. W. (1952). Pupil Size as determined by adapting luminance. *Journal of the Optical Society of America, 42*, 492–495.

DeValois, R. L., & DeValois, K. K. (1975). Neural coding of color. In E. D. Carterette & M. P. Friedman (Eds.), *Handbook of perception, V*. New York: Academic Press.

DeValois, R. L., & DeValois, K. K. (1988). *Spatial vision*. New York: Oxford University Press.

Fach, C., & Sharpe, L. T. (1986). Assimilative hue shifts in color gratings depend on bar width. *Perception & Psychophysics, 40*, 412–418.

Festinger, L., Coren, S., & Rivers, G. (1970). Effect of attention on brightness contrast and assimilation. *American Journal of Psychology, 83*, 189–207.

Fuchs, W. (1923). Experimentelle Untersuchungen über die Änderung von Farben unter dem Einfluss von Gestalten (Angleichungsercsheinungen) (Experimental investigations on the alteration of color under the influence of Gestalten). *Zeitschrift für Psychologie*(92), 249–325.

Helson, H. (1963). Studies of anomalous contrast and assimilation. *Journal of the Optical Society of America, 53*, 179–184.

Humanski, R. A., & Wilson, H. R. (1992). Spatial frequency mechanisms with short-wavelength-sensitive cone inputs. *Vision Research, 32*, 549–560.

Hurvich, L. M. (1981). *Color vision*. Sunderland, MA: Sinauer Association.

Hurvich, L. M., & Jameson, D. (1974). Opponent processes as a model of neural organization. *American Psychologist, 29*, 88–102.

Jameson, D., & Hurvich, L. M. (1955). Some quantitative aspects of an opponent-colors theory I. Chromatic responses and spectral saturation. *Journal of the Optical Society of America, 45*, 546–552.

Jameson, D., & Hurvich, L. M. (1989). Essay concerning color constancy. *Annual Review of Psychology, 40*, 1–22.

Johnson, E. N., Hawken, M. J., & Shapley, R. (2001). The spatial transformation of color in the primary visual cortex of the macaque monkey. *Nature Neuroscience, 4*, 409–416.

Kaiser, P. K., & Boynton, R. M. (1996). *Human color vision* (2nd ed.). Washington, DC: Optical Society of America.

King, D. L. (1988). Assimilation is due to one perceived whole and contrast is due to two perceived wholes. *New Ideas in Psychology*, 277–288.

Longere, P., Shevell, S. K., & Knoblauch, K. (2000). Color assimilation: Effect of spatial statistics. *Investigative Ophthalmology & Visual Science, 41*, S805.

MacLeod, D. I. A., & Boynton, R. M. (1979). Chromaticity diagram showing cone excitation by stimuli of equal luminance. *Journal of the Optical Society of America, 69*, 1183–1185.

Marimont, D. H., & Wandell, B. A. (1994). Matching color images: The effects of axial chromatic aberration. *Journal of the Optical Society of America A, 11*, 3113–3122.

Monnier, P., & Shevell, S. K. (2004). Chromatic induction from S-cone patterns. *Vision Research, 44*, 849–856.

Moulden, B., Kingdom, F., & Wink, B. (1993). Colour pools, brightness pools, assimilation, and the spatial resolving power of the human colour-vision system. *Perception, 22*, 343–351.

Rice, J. A. (1995). *Mathematical statistics and data analysis* (2nd ed.). Belmont, CA: Wadsworth Publishing Co.

Shevell, S. K. (2003). Color appearance. In S. K. Shevell (Ed.), *The science of color* (pp. 149–190). Oxford, UK: Elsevier.

Shevell, S. K., & Cao, D. (2003). Chromatic assimilation: Evidence for a neural mechanism. In J. Mollon, J. Pokorny, & K. Knoblauch (Eds.), *Normal and defective colour vision* (pp. 114–121). Oxford, UK: Oxford University Press.

Shevell, S. K., & Wei, J. (1998). Chromatic induction: Border contrast or adaptation to surrounding light? *Vision Research, 38*, 1561–1566.

Smith, V. C., Jin, P. Q., & Pokorny, J. (2001). The role of spatial frequency in color induction. *Vision Research, 41*, 1007–1021.

Tansley, B. W., & Boynton, R. M. (1978). Chromatic border perception: The role of red- and green-sensitive cones. *Vision Research, 18*, 683–697.

Taya, R., Ehrenstein, W. H., & Cavonius, C. R. (1995). Varying the strength of the Munker-White effect by stereoscopic viewing. *Perception, 24*, 685–694.

Todorovic, D. (1997). Lightness and junctions. *Perception, 26*, 379–394.

von Bezold, W. (1876). *The theory of color in its relation to art and art-industry*. Boston: Prang.

von Kries, J. (1905). Influence of adaptation on the effects produced by luminous stimuli. In D. L. MacAdam (Ed.). *Sources of color science* (Vol. 124). Cambridge, MA: MIT Press.

Walker, J. T. (1978). Brightness enhancement and the Talbot level in stationary gratings. *Perception and Psychophysics, 23*, 356–359.

Ware, C., & Cowan, W. B. (1982). Changes in perceived color due to chromatic interactions. *Vision Research, 22*, 1353–1362.

Williams, D. R., Brainard, D. H., McMahon, M. J., & Navarro, R. (1994). Double-pass and interferometric measures of the optical quality of the eye. *Journal of the Optical Society of America A, 11*, 3123–3135.

Wright, W. D. (1969). *The measurement of color*. London: Hilger.

Zaidi, Q., Spehar, B., & Shy, M. (1997). Induced effects of backgrounds and foregrounds in three-dimensional configurations: The role of T-junctions. *Perception, 26*, 395–408.